Magnetism of two-dimensional defects in Pd: Stacking faults, twin boundaries, and surfaces

Simone S. Alexandre and Eduardo Anglada
Departamento de Física de la Materia Condensada, Universidad Autónoma de Madrid, 28049 Madrid, Spain

José M. Soler and Félix Yndurain*
Departamento de Física de la Materia Condensada, Universidad Autónoma de Madrid, 28049 Madrid, Spain
and Instituto de Ciencia de Materiales Nicolás Cabrera, Universidad Autónoma de Madrid, 28049 Madrid, Spain
(Received 30 January 2006; published 3 August 2006)

Careful first-principles density functional calculations reveal the importance of hexagonal versus cubic stacking of close-packed planes of Pd as far as local magnetic properties are concerned. We find that, contrary to the stable face-centered-cubic phase, which is paramagnetic, the hexagonal-close-packed phase of Pd is ferromagnetic with a magnetic moment of 0.35 μ_B/atom. Our results show that two-dimensional defects with local hcp stacking, like twin boundaries and stacking faults, in the otherwise fcc Pd structure, increase the magnetic susceptibility. The (111) surface also increases the magnetic susceptibility and it becomes ferromagnetic in combination with an individual stacking fault or twin boundary close to it. On the contrary, we find that the (100) surface decreases the tendency to ferromagnetism. The results are consistent with the magnetic moment recently observed in small Pd nanoparticles, with a large surface area and a high concentration of two-dimensional stacking defects.

DOI: 10.1103/PhysRevB.74.054405 PACS number(s): 75.75.+a, 73.22.−f, 75.50.Cc

I. INTRODUCTION

Despite their narrow *d* bands and high densities of states (DOS) at the Fermi level, which favor magnetism, there are only three ferromagnetic transition metals in nature. Palladium is paramagnetic in its stable face-centered-cubic (fcc) structure, but with a very high magnetic susceptibility. Several calculations have shown that its Fermi level lies just above a large peak in the DOS, at the top of the *d* bands. The DOS at the Fermi level, of ~1.1 states per spin, eV, and atom (Chen *et al.*[1] and references therein) is almost high enough, but not quite so, to fulfill the Stoner criterion for itinerant magnetism, since the Stoner exchange parameter is ~0.73 eV.[2,3] The calculations have also shown that Pd, in its fcc crystal structure, becomes ferromagnetic by increasing the lattice constant by just a few percent.[4] All these results have stressed the subtle balance of magnetism in Pd.

Therefore, we suggest that variations in the atomic arrangement can induce changes in the density of states at the Fermi level, which, in turn, can induce magnetism. In this direction, it has been proposed that monatomic Pd nanowires are ferromagnetic, in either their energetic[5,6] or thermodynamic[7] equilibrium length. Also, recent experimental results[8] indicate that fcc Pd nanoparticles with stacking faults and twin boundaries present ferromagnetism. Other experiments[9] on small Pd nanoparticles also indicate the existence of a hysteresis loop which, in this case, is interpreted as due to a nonzero magnetic moment at the (100) surface atoms.

Stacking faults and twin boundaries are very common two-dimensional defects in fcc metals as well as in diamond and wurtzite-structure semiconductors. Their abundance is partly due to their low energy of formation, since they preserve the local geometry and close packing. Their importance in the mechanical properties, like hardness and brittleness, have been recognized for many years. Recently, the role played by the stacking of (111) layers has been emphasized in connection with the magnetic orientation and magnetic ordering of thin layers and superlattices of magnetic metals.[10–12] The growth of Co on top of the Cu (111) surface has been extensively studied experimentally, and the correlation between stacking pattern and magnetic properties has been reasonably well established.

At this stage it seems worth studying the effect of the stacking sequences and of the surfaces on the electronic and magnetic properties of Pd. With these ideas in mind, we have calculated total energies and magnetic moments of Pd in both the fcc and hexagonal-close-packed (hcp) phases, as well as in surfaces and near two-dimensional stacking defects like intrinsic and extrinsic stacking faults, and twin boundaries.

II. METHODOLOGY

All our calculations are performed within density functional theory[13] (DFT), using either the local density approximation[14] (LDA) or the generalized gradient approximation[15] (GGA) to exchange and correlation. Most of the calculations were obtained with the SIESTA[16,17] method, which uses a basis of numerical atomic orbitals[18] and separable[19] norm-conserving pseudopotentials[20] with partial core corrections.[21] To generate the pseudopotentials and basis orbitals, we use a Pd configuration $4d^9 5s^1$, since we have checked that it leads to better transferability and bulk properties than the ground-state configuration $4d^{10}5s^0$. After several tests we have found satisfactory the standard double-ζ basis with polarization orbitals (DZ+P) which has been used throughout this work. The convergence of other precision parameters was carefully checked. The range of the atomic basis orbitals was obtained using an energy shift[17] of 50 meV. The real-space integration grid had a cutoff of 500 Ry, while around 9000 *k*-points/atom^{-1} were used in the Brillouin zone sampling. To accelerate the self-consistency

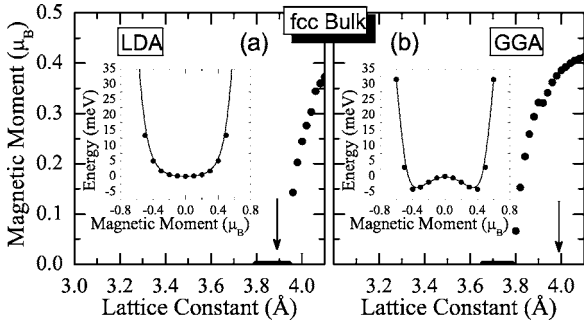

FIG. 1. Magnetic moment versus lattice constant for fcc Pd obtained with the SIESTA code and the LDA and GGA functionals. The insets indicate the variation of the total energy with magnetic moment at the corresponding equilibrium lattice constants, indicated by arrows.

convergence, a broadening of the energy levels was performed using the method of Methfessel and Paxton[22] which is very suitable for systems with a large variation of the density of states at the vicinity of the Fermi level.

It is necessary to mention that most of the energy differences between paramagnetic and ferromagnetic solutions in Pd structures are extremely small, which requires a very high convergence in all precision parameters and tolerances and especially in the number of k points. It must be recognized, however, that the basic DFT uncertainty is probably larger than those energy differences, so that it is not really possible to determine reliably whether a particular defect or structure is paramagnetic or ferromagnetic. Still, we think that it is possible to find reliably the relative tendency towards magnetism of different structures. In particular, $E(M)$ curves, of total energy versus total magnetic moment, provide an excellent tool to study the tendency to magnetism in different systems: independently of whether the systems are paramagnetic or ferromagnetic, one may determine if a defect or a surface has a smaller or a larger tendency to magnetism than the bulk, depending on which of the two $E(M)$ curves is higher. In addition, the self-consistent convergence is considerably faster at constant magnetic moment, so that it is possible to determine reliably (for a given functional) relative energies as small as a fraction of an meV.

III. BULK CRYSTALS

The first mandatory system to be considered is the perfect bulk crystal in its experimentally stable fcc phase. In principle, the GGA functional goes beyond the LDA and it is generally considered to be more accurate and reliable. However, in the case of Pd, we find that the GGA gives a lattice constant of 3.99 Å, 2.5% larger than experiment, and a ferromagnetic ground state with a magnetic moment of $0.4\mu_B$/atom and an energy 4.5 meV/atom below the paramagnetic phase (Fig. 1). Since this energy difference is very small and to rule out the possibility that the ferromagnetic phase is favored by the pseudopotential or basis set used, we have reproduced[6] this result using two other DFT methods: the pseudopotential plane-wave code VASP[23] and the all-electron augmented plane-wave method WIEN,[24] both with the same GGA functional.[15] Previous GGA calculations by Singh and Ashkenazi,[25] using a different functional, also found a lattice constant larger than the experimental one, but did not address the subtle ferromagnetic-paramagnetic transition with sufficient detail.

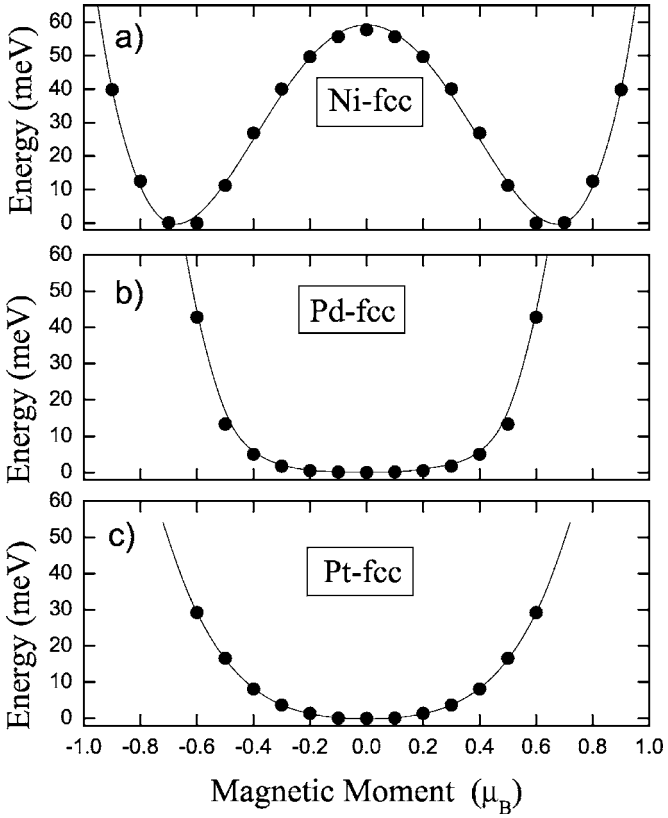

FIG. 2. Total energy versus magnetic moment for three transition metals in the same column of the periodoc table, calculated in the LDA. Note the flatness of the Pd curve, responsible for the large magnetic susceptibility of this metal.

On the other hand, within the LDA we find a paramagnetic ground state and a lattice constant of 3.89 Å, both in agreement with the experimental values and with previous LDA calculations of Moruzzi and Marcus.[4] These results suggest that the GGA is not necessarily more reliable to study magnetism in Pd. In fact, it is not feasible to study the possible existence of magnetic defects in fcc Pd when the bulk result is already ferromagnetic. Therefore, we have chosen the spin-dependent LDA to perform most of the remaining calculations in this work, although GGA results have been obtained also as a check in some cases.

The magnetic susceptibility χ of the magnetic moment M to an external magnetic field H is

$$\chi = \left(\frac{\partial M}{\partial H}\right)_{H=0} = \left(\frac{\partial^2 E}{\partial M^2}\right)^{-1}_{M=0}.$$

Thus, the flatness of the $E(M)$ curve in Fig. 1 implies a very large susceptibility, even within the LDA. To compare with the other transition metals in the same column of the periodic table we have calculated the variation of energy with magnetic moment for Ni and Pt. The results are shown in Fig. 2.

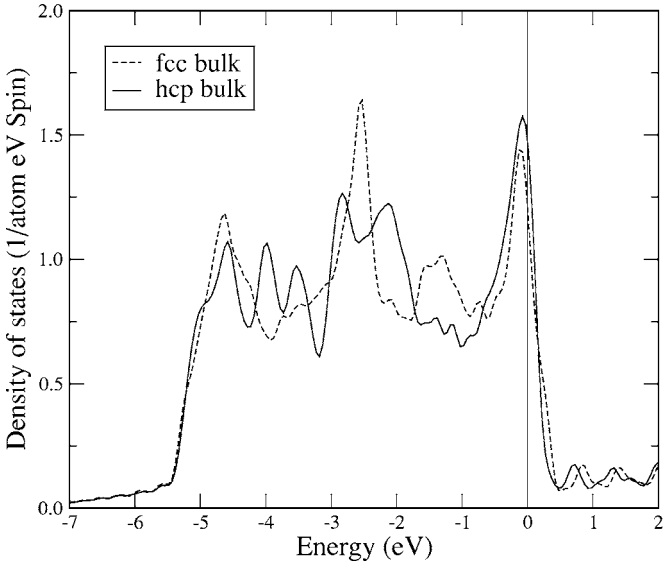

FIG. 3. Calculated electronic densities of states of Pd in the paramagnetic phase (i.e., forcing equal spin-up and spin-down populations) in the fcc and hcp crystal structures. The vertical line indicates the Fermi level.

We immediately observe a clear ferromagnetic and paramagnetic behavior of Ni and Pt respectively, while Pd, as indicated above, is paramagnetic but very close to the ferromagnetic transition.

In order to study how magnetism depends on the local geometry and stacking of atoms, we have first considered the hcp structure as compared to the fcc one. It is known that the breaking of the cubic symmetry in stacking faults, while keeping the number of nearest-neighbor atoms and their bond lengths and angles, induces a rearrangement of the d energy bands that can even give rise to localized electronic states.[26] The DOS of hcp and fcc structures, in the paramagnetic phase, shown in Fig. 3, were calculated for the same nearest-neighbor distance of 2.76 Å and the ideal ratio $c/a=(8/3)^{1/2}$ for the hcp structure, since we obtain that both structures are stable at this distance, with the hcp c/a ratio only 0.75% larger than the ideal value. Several points are worth mentioning: (i) The d band width is almost identical in both structures because they have identical nearest-neighbor configurations. (ii) The shapes of the DOS are very different, as a consequence of the breaking of the cubic symmetry: in fcc the second-nearest-neighbor atoms are staggered whereas in hcp they are eclipsed and the lack of cubic symmetry inhibits the t_{2g}-e_g splitting of the d bands. (iii) The DOS at the Fermi level is larger in hcp than in fcc (1.43 versus 1.15 states per atom per eV and per spin). This implies that Pd in the hcp structure satisfies the Stoner condition for ferromagnetism: with a Stoner exchange parameter $I=0.73$ eV,[2,3] we get $I\times D(E_F)=0.84$ for fcc and $I\times D(E_F)=1.05$ for hcp.

We have then calculated the total energy and the magnetic order in the hcp phase in the LDA. The results are shown in Fig. 4. We immediately observe that, contrary to what happens in the fcc structure, there is a nonzero magnetic moment of $0.35\mu_B$/atom at the equilibrium interatomic separation for the hcp structure, $d=2.76$ Å. Like in the fcc phase, the system is close to a magnetic-nonmagnetic transition but, in this case, in the ferromagnetic side, with the ferromagnetic hcp phase approximately 1.7 meV lower in energy than the paramagnetic one. The transition from paramagnetism to ferromagnetism, as a function of the lattice constant, is abrupt, like in the fcc case, although we cannot assess with enough confidence whether it is first or second order.[4,27]

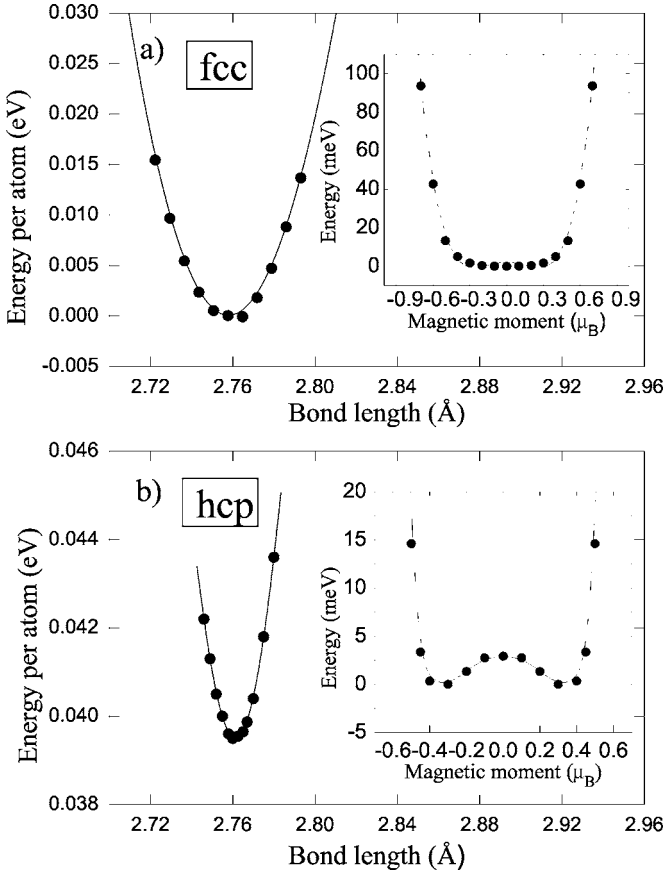

FIG. 4. Calculated total energy for (a) fcc and (b) hcp Pd as a function of the nearest-neighbor distance. The insets at (a) and (b) show the total energy versus magnetic moment for the fcc and hcp structures, respectively. In these cases the energy origin is at the corresponding minima.

Finally, the hcp structure is 4.0 meV higher in energy than the fcc. This ordering is in agreement with experiment, and we reproduce it also with the GGA, but it is in contradiction with the calculations of Huger and Osuch[28] that reported an hcp structure lower in energy, but also ferromagnetic.

IV. BULK DEFECTS

Hexagonal- (111) close-packed planes of atoms can be stacked in different ways, giving rise to different structures. If we label the three possible positions of the atoms as A, B, and C, the fcc stacking is …$ABCABC$… and that of hcp is …$\underline{ABABAB}$…,[29] where the layers with hexagonal symmetry are underlined. Different defects can be generated in the fcc structure: The intrinsic and extrinsic stacking faults have two hexagonal layers, with stacking sequences …$ABC\underline{AC}ABC$… and …$ABC\underline{A}C\underline{B}CABC$… respectively. The twin boundary

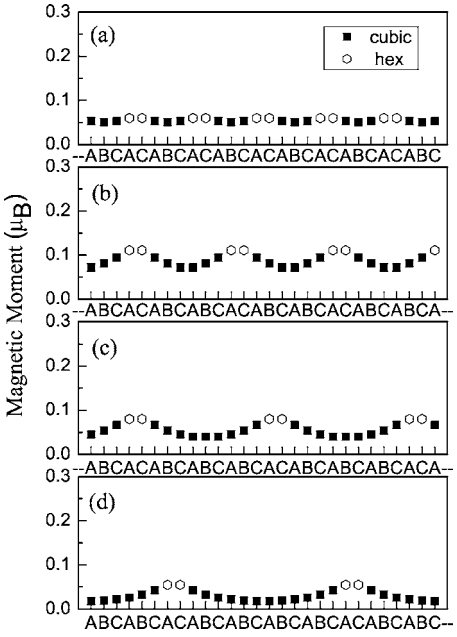

FIG. 5. Local magnetic moment in supercells of different thickness, containing a single intrinsic stacking fault between fcc layers, calculated with the LDA.

has a single hexagonal layer with …*ABCACBA*… stacking.

Previous model calculations[26] at stacking faults of transition metals indicate an important perturbation of the local densities of states from that of the perfect fcc lattice. The presence of a hexagonal stacking of layers induces localized electronic states[26,30] and an enhancement of the DOS at the top of the valence band. These calculations suggest possible variations of the magnetic properties around the extended defect. We have performed calculations of several packing sequences, in supercells containing various numbers of fcc layers, to study to what extent different local configurations can give rise to magnetic moments. The results of the calculations, both in the perfect crystals and in the defects, are independent (within less than 1%) of the initial input moment.

Most of the calculated supercells have a finite magnetic moment and some are shown in Fig. 5. However, its variation with the supercell thickness is rather complex and nonmonotonic. We suspect that this complex behavior is due to an oscillatory component of the magnetic coupling between the neighboring stacking faults, like that observed in superstructures of magnetic slabs sandwiched between nonmagnetic metals.[31] Although we have not been able to stabilize any antiferromagnetic solution in double-size supercells, this may be due to the size limitations and to the difficulties of convergence. As expected, the magnetic moments are smaller in fcc than in hcp layers, but they are nevertheless far from negligible. The interplay between the magnetism of the hexagonal layers and the paramagnetism of the cubic ones, both close to a paramagnetic to ferromagnetic transition, is very subtle. What is important is that the hexagonal layers have a tendency to become magnetic and they induce magnetic moments at the atoms in the cubic layers. This is due, first, to the large magnetic susceptibility in fcc Pd, where the hexagonal layers act as magnetic impurities. And second, because of the two-dimensional character of the defects, any magnetic perturbation decays very slowly with distance, like in a pseudo-one-dimensional metal. In other words, there is a long-range RKKY-like interaction between the hcp layers through the intermediate fcc ones.

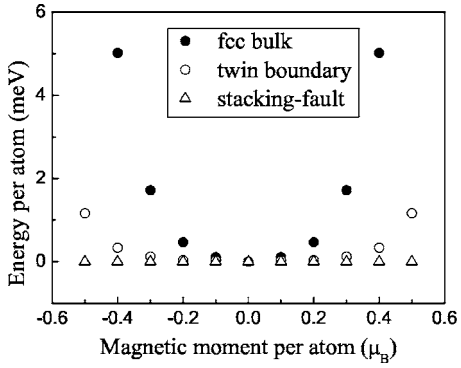

FIG. 6. Total energy as a function of the magnetic moment for differents two-dimensional defects of Pd, with local hexagonal symmetry, compared to the bulk fcc lattice. The energy at $M=0$ has been shifted to a common value. The defects are separated by six fcc layers like in Fig. 5(b). The stacking fault curve has a minimum of -0.2 meV at $M \simeq 0.09 \mu_B$/atom, in agreement with Fig. 5(b), which is not noticeable at the figure scale.

Given the size limitations of our calculated supercells and the nonmonotonic magnetic moment with increasing supercell thickness, it is not possible to conclude confidently whether isolated planar defects in fcc Pd have a finite magnetic moment, within the LDA. However, Fig. 6 clearly shows that all the hexagonal defects have a larger tendency to magnetism than the bulk fcc lattice, as indicated by their respective $E(M)$ curves. This is hardly surprising, given the ferromagnetic character of hcp Pd. On the other hand, all the supercells are, of course, strongly magnetic within the GGA, with a larger tendency to magnetism [lower $E(M)$ curve] than the bulk fcc crystal. Therefore, it is perfectly possible that an isolated stacking fault in fcc Pd is indeed magnetic in nature.

V. SURFACES

Recent experimental results[9] on Pd nanoparticles have been interpreted as magnetism at (100) surfaces. In principle, surface magnetism is plausible in general because the lower coordination of surface atoms favors narrower bands and larger densities of states. In practice, however, surface relaxation and reconstruction may contract the surface bond lengths and more than compensate for the lower coordination. We have then calculated the electronic structure of finite Pd slabs in the (100) and (111) orientations, after carefully relaxing their geommetry. The results of the calculated total energy versus magnetic moment are shown in Fig. 7 for the largest calculated thickness. This general tendency is consistently obtained for sufficiently thick slabs, but the thickness dependence of the total magnetic moment, shown in Fig. 8, is not monotonic, as in the bulk supercells.

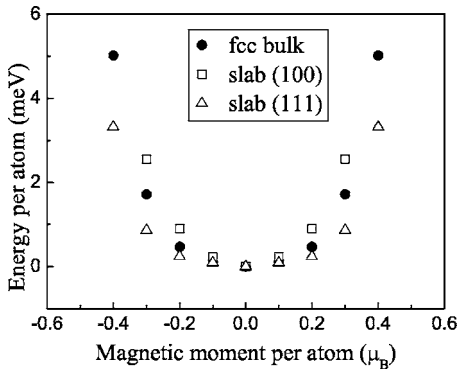

FIG. 7. Total energy within the LDA versus magnetic moment of bulk fcc Pd and of nine-layer slabs with surfaces oriented in the (100) and (111) directions. The energy at $M=0$ has been shifted to a common value.

We observe in Fig. 7 that the minimum energy is at zero magnetic moment and therefore the two surfaces are paramagnetic. Moreover, the $E(M)$ curve of the (100) surface is higher than that of the bulk, showing that this surface is less prone to magnetism than the bulk. On the other hand, the (111) surface, although also paramagnetic within the LDA, has a larger susceptibility than the bulk, which makes it plausible that it may be magnetic in nature.

We have found that bulk planar defects, as well as (111) surfaces, have a larger tendency to magnetism than the bulk Pd crystal, which is itself on the verge of ferromagnetism. Since both surfaces and defects are in high concentrations in nanoparticles and both have in fact been proposed independently[8,9] as responsible for the observed magnetic moment of these particles, it makes sense to consider their combined effect. To this end, we have calculated the geometry, energy, and magnetism of planar defects close to a (111) surface. We use a slab in which the opposite surface is "magnetically passivated" by imposing a short distance between the first two atomic planes, what immediately destroys their local magnetic moment. In this way, we ensure that the possible magnetic moment of the slab is due to the combination of the stacking fault and a single surface (in fact, this structure penalizes and sets a lower limit for the appearence of magnetism). Still, as shown in Fig. 9, we find a clear magnetic moment in all the cases considered. This tendency is further demonstrated by their $E(M)$ curves, presented in Fig. 10 for two cases, which show unambiguously their magnetic character. Furthermore, the total energy of all the slabs is lower than that of the defects in the bulk, plus that of the unfaulted slab, implying that the surface attracts the defects and that they should therefore be expected to appear together in nanoparticles, due to the high concentration of stacking faults and to the small space between surfaces. Notice that the extrinsic stacking fault is more stable than the intrinsic one both at the surface and at the bulk.

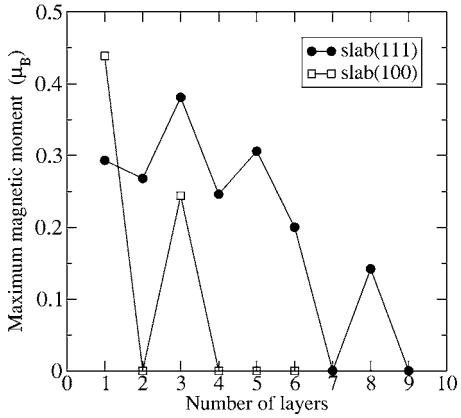

FIG. 8. Largest local magnetic moment, as a function of the number of layers, in slabs with surfaces oriented in the (100) and (111) directions.

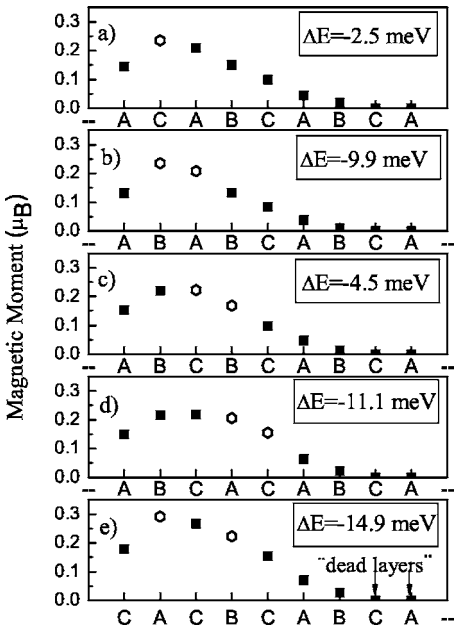

FIG. 9. Local magnetic moments for different stackings of hexagonal and cubic planes in a slab of nine layers. (a) Twin boundary. (b), (c), and (d) Intrinsic stacking faults, with the hcp layers in differents positions. (e) Extrinsic staking fault. Squares and hexagons represent cubic and hexagonal layers, respectively. The distance between the two rightmost layers was fixed to a small value, in order to destroy their tendency to magnetism and thus to simulate the bulk. The energies reported are the difference between the total energy of the slab, minus those of the defect in the bulk and of the unfaulted slab. The formation energies in the bulk are 33.9, 74.7, and 73.0 meV for the twin boundary, intrinsic stacking fault, and extrinsic stacking fault, respectively.

VI. CONCLUSIONS

Our main conclusions can be summarized as follows: (i) The GGA functional gives an incorrect ferromagnetic ground state for the fcc Pd crystal. Accordingly, all the defects studied are also magnetic within the GGA but, obviously, this does not imply that they are magnetic in nature. On the contrary, the simpler LDA gives the correct lattice constant and paramagnetic state. (ii) The hcp phase is ferromagnetic, within both the LDA and GGA. In the LDA, it has an energy 1.7 meV lower than the hcp paramagnetic state and 4.0 meV

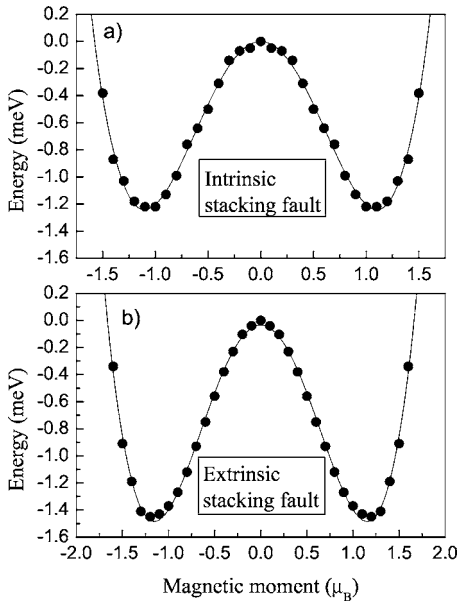

FIG. 10. Calculated total energy, as a function of the magnetic moment, for two different two-dimensional defects close to a (111) surface [shown in Figs. 9(c) and 9(e)].

above the fcc phase. (iii) We cannot determine whether an isolated stacking fault is magnetic in the LDA, but it certainly has a larger magnetic susceptibility than the perfect crystal and might be magnetic in nature, given the uncertainty between the different functionals. (iv) The free (100) surface is paramagnetic, with a lower susceptibility than the bulk crystal. (v) The (111) surface is paramagnetic in the LDA, but it has a larger susceptibility than the bulk crystal, and it might be magnetic in nature. (vi) Hexagonal planar defects are attracted towards a (111) surface, and they become clearly magnetic when close enough.

Therefore, (100) surfaces are not good candidates as the origin of magnetism in Pd nanoparticles, as they had been proposed.[9] In contrast, planar stacking defects, (111) surfaces, and especially a combination of both are plausible candidates to present permanent magnetic moments and to be responsible for the magnetism observed in Pd nanoparticles. Thus, our results are consistent with experiments in small Pd clusters of average diameter 2.4 nm, which are reported to display spontaneous magnetization.[8] High-resolution transmission electron microscopy has shown that a high percentage of the particles exhibit single and multiple twinning boundaries. In addition, the smallness of the spontaneous magnetization seems to indicate that only a small fraction of atoms hold a permanent magnetic moment and contribute to ferromagnetism. Other experimental results[9] on small Pd particles have also shown their ferromagnetic character. Besides, ferromagnetism can also take place in other non ideal structures like nanowires.[5]

Magnetic anomalies observed experimentally in different Ni (Ref. 32) and Co (Ref. 12) stacking can be interpreted along the lines described in this work. The fact that stacking faults in Pd display non-negligible magnetic moments, not present in bulk fcc crystal, opens new lines of research. The appearance of magnetism in nominal fcc samples should be reexamined in view of our results, since so far the possibility of magnetism around stacking faults has been overlooked. Also, layer growth of Pd on top of nonmagnetic substrates, including Pd itself, may produce an interesting magnetic phenomenology in connection with the stacking structure which, in turn, depends on the method used for growth. The study of the dependence of the magnetic properties of Pd-grown Ag(111) and Pd/Ag multilayers on the stacking sequences is under way and will be reported elsewhere.

ACKNOWLEDGMENTS

We would like to thank A. Hernando, who brought our attention to this problem, to Ó. Paz for his assistance in the technical part of this work, and to M. Mattesini for his help in the plane-wave basis calculations. Work supported Spain's Ministery of Science through Grants No. BFM2002-10510-E and No. BFM2003-03372.

*Electronic address: felix.yndurain@uam.es

[1] H. Chen, N. E. Brener, and J. Callaway, Phys. Rev. B **40**, 1443 (1989).
[2] J. F. Janak, Phys. Rev. B **16**, 255 (1977).
[3] N. Takano, T. Kai, K. Shiiki, and F. Terasaki, Solid State Commun. **97**, 153 (1996).
[4] V. L. Moruzzi and P. M. Marcus, Phys. Rev. B **39**, 471 (1989).
[5] A. Delin, E. Tosatti, and R. Weht, Phys. Rev. Lett. **92**, 057201 (2004).
[6] S. S. Alexandre, M. Mattesini, J. M. Soler, and F. Yndurain, Phys. Rev. Lett. **96**, 079701 (2006).
[7] E. Tosatti, S. Prestipino, S. Kostlmeier, A. Dal Corso, and F. D. Di Tolla, Science **291**, 288 (2001).
[8] B. Sampedro, P. Crespo, A. Hernando, R. Litran, J. C. Sanchez Lopez, C. Lopez Cartes, A. Fernandez, J. Ramirez, J. Gonzalez Calbet, and M. Vallet, Phys. Rev. Lett. **91**, 237203 (2004).
[9] T. Shinohara, T. Sato, and T. Taniyama, Phys. Rev. Lett. **91**, 197201 (2003).
[10] S. S. P. Parkin, R. F. Marks, R. F. C. Farrow, G. R. Harp, Q. H. Lam, and R. J. Savoy, Phys. Rev. B **46**, 9262 (1992).
[11] M. Zheng, J. Shen, J. Barthel, P. Ohresser, Ch. V. Mohan, and J. Kirchner, J. Phys.: Condens. Matter **12**, 783 (2000).
[12] O. Pietzsch, A. Kubetzka, M. Bode, and R. Wiesendanger, Phys. Rev. Lett. **92**, 057202 (2004).
[13] W. Kohn and L. J. Sham, Phys. Rev. **140**, A1133 (1965).
[14] J. P. Perdew and A. Zunger, Phys. Rev. B **23**, 5048 (1981).
[15] J. P. Perdew, K. Burke, and M. Ernzerhof, Phys. Rev. Lett. **77**, 3865 (1996).
[16] P. Ordejón, E. Artacho, and J. M. Soler, Phys. Rev. B **53**, R10441 (1996).
[17] J. M. Soler, E. Artacho, J. D. Gale, A. Garcia, J. Junquera, P. Ordejon, and D. Sanchez-Portal, J. Phys.: Condens. Matter **14**,

2745 (2002).
[18] O. F. Sankey and D. J. Niklewski, Phys. Rev. B **40**, 3979 (1989).
[19] L. Kleinman and D. M. Bylander, Phys. Rev. Lett. **48**, 1425 (1982).
[20] N. Troullier and J. L. Martins, Phys. Rev. B **43**, 1993 (1991).
[21] S. G. Louie, S. Froyen, and M. L. Cohen, Phys. Rev. B **26**, 1738 (1982).
[22] M. Methfessel and A. T. Paxton, Phys. Rev. B **40**, 3616 (1989).
[23] G. Kresse and J. Furthmuller, Phys. Rev. B **54**, 11169 (1996).
[24] P. Blaha, K. Schwarz, G. K. H. Madsen, D. Kvasnicka, and J. Luitz, Computer code WIEN2K, an augmented plane wave + local orbitals program for calculating crystal properties, Technical Universität Wien, Austria, 2001.
[25] D. J. Singh and J. Ashkenazi, Phys. Rev. B **46**, 11570 (1992).
[26] F. Yndurain and L. M. Falicov, Phys. Rev. Lett. **37**, 928 (1976).
[27] V. L. Moruzzi, Phys. Rev. Lett. **57**, 2211 (1986).
[28] E. Huger and K. Osuch, Europhys. Lett. **63**, 90 (2003).
[29] C. Kittel, *Introduction to Solid State Physics* (Wiley, New York, 1996).
[30] A. L. Vázquez de Parga, F. J. García-Vidal, and R. Miranda, Phys. Rev. Lett. **85**, 4365 (2000).
[31] P. Bruno and C. Chappert, Phys. Rev. Lett. **67**, 1602 (1991).
[32] O. Robach, C. Quiros, H. Isern, P. Steadman, K. F. Peters, and S. Ferrer, Phys. Rev. B **67**, 220405(R) (2003).